Journal of Nepal Geological Society, 2013, Vol. 46, pp. 143-162

FE model of the Suez rift basin and its geodynamic implications

***Sunil Kumar Dwivedi[1] and Daigoro Hayashi[2]**

[1]Central Department of Geology, Tribhuvan University, Kirtipur, Kathmandu, Nepal
[2]Simulation Tectonics Laboratory, Faculty of Science, University of the Ryukyus, Okinawa, 903-0213, Japan
*(*Email: sunildwd@gmail.com)*

ABSTRACT

Northeast Africa forms the northernmost extension of the East African Rift System and is considered one of the geodynamically active regions in the Earth. The Red Sea, Gulf of Suez, Gulf of Aqaba, and Dead Sea transform are the most prominent tectonic features in the region. Despite the motion of African and Arabian Plates being well-established, contribution of these plates to the origin of stress field in the Gulf of Suez has been under discussion. The main debate is on the controlling factors for the geodynamic origin of the Suez rift basin. The factors, either the present-day stress field is originated due to the Gulf of Suez rift itself or due to the influence of nearby tectonic boundaries, is under question. An attempt has been made to model the stress field of the area by 2D plane stress finite-element (FE) modeling incorporating realistic rock parameters and velocities for African and Arabian Plates. The modeled maximum horizontal stress (σ_{Hmax}) and minimum horizontal stress (σ_{hmin}) directions correlate well with observed stress indicators from the world stress map (WSM), focal mechanism solutions (FMS) of earthquakes, in-situ stress measurements, and geological stress information; and displacement field correlate well with GPS data of the region. Modeling result reveals that the present-day stress field in the Gulf of Suez is emerged from coeval influence of superimposed forces acting from rifting processes in the Red Sea, Gulf of Aqaba, and Dead Sea transform.

Key words: Africa, Suez rift, stress field, finite-element modeling, geodynamics

Received: 15 May, 2013 **Revision accepted**: 25 June, 2013

INTRODUCTION

The geology, tectonics, and active deformation of northeast Africa are largely affected by complex interactions between the African and Arabian Plates. Their relative motions have allowed rifting in the Red Sea, Gulf of Suez, and Gulf of Aqaba with a left lateral movement along the Dead Sea transform (McKenzie 1972; Joffe and Garfunkel 1987; DeMets et al. 1990; 1994; Girdler 1991; Guiraud and Bosworth 1999; Dwivedi and Hayashi 2009; Dwivedi and Hayashi 2010; Dwivedi and Hayashi 2011; Morsy et al. 2012) (Fig. 1). As a result, most of the available earthquake focal mechanisms show normal and strike-slip type motion near these tectonic boundaries, which support the divergence of these plates.

Modeling crustal stress field is the key to understanding physical processes acting within the Earth's crust. Northeast Africa provides an ideal area to study short-scale variation of stress field since the stress data are readily available (Zoback 1992; Badawy and Horv´ath 1999a; Badawy 2001; Mahmoud 2003; Mahmoud et al. 2005; Riguzzi et al. 2006; Heidbach and Ben-Avraham 2007; Heidbach et al. 2010). Despite the motion of African and Arabian Plates being well-established, contribution of these plates to the origin of stress field in the Gulf of Suez is under discussion (Steckler and ten Brink 1986; Steckler et al. 1988; Lyberis 1988; Bosworth and Taviani 1996; Bosworth and Steckler 1997; Taha and Miguel 2008). Earthquake focal mechanisms, in-situ stress measurements, geological stress information, and geodetic observations have provided an evidence for a recent change in state of stress and stress regime in the region (Bosworth and Taviani 1996; Bosworth and Strecker 1997; Badawy 2001, 2005; Mahmoud 2003; Wdowinski et al. 2004; El-Fiky 2005; Mahmoud et al. 2005; Hussein et al. 2006; Riguzzi et al. 2006; Gomez et al. 2007; Heidbach and Ben-Avraham 2007; Abdel-Rahman et al. 2009; Heidbach et al. 2010; Morsy et al. 2012). Tectonically, opening of the Red Sea began in Oligocene-Early Miocene due to the differential motion between African and Arabian Plates in the south (Ghebreab 1998) that subsequently led the opening of Gulf of Suez in the north (Omar and Steckler 1995). Later, in Middle Miocene the opening of the Gulf of Suez slowed

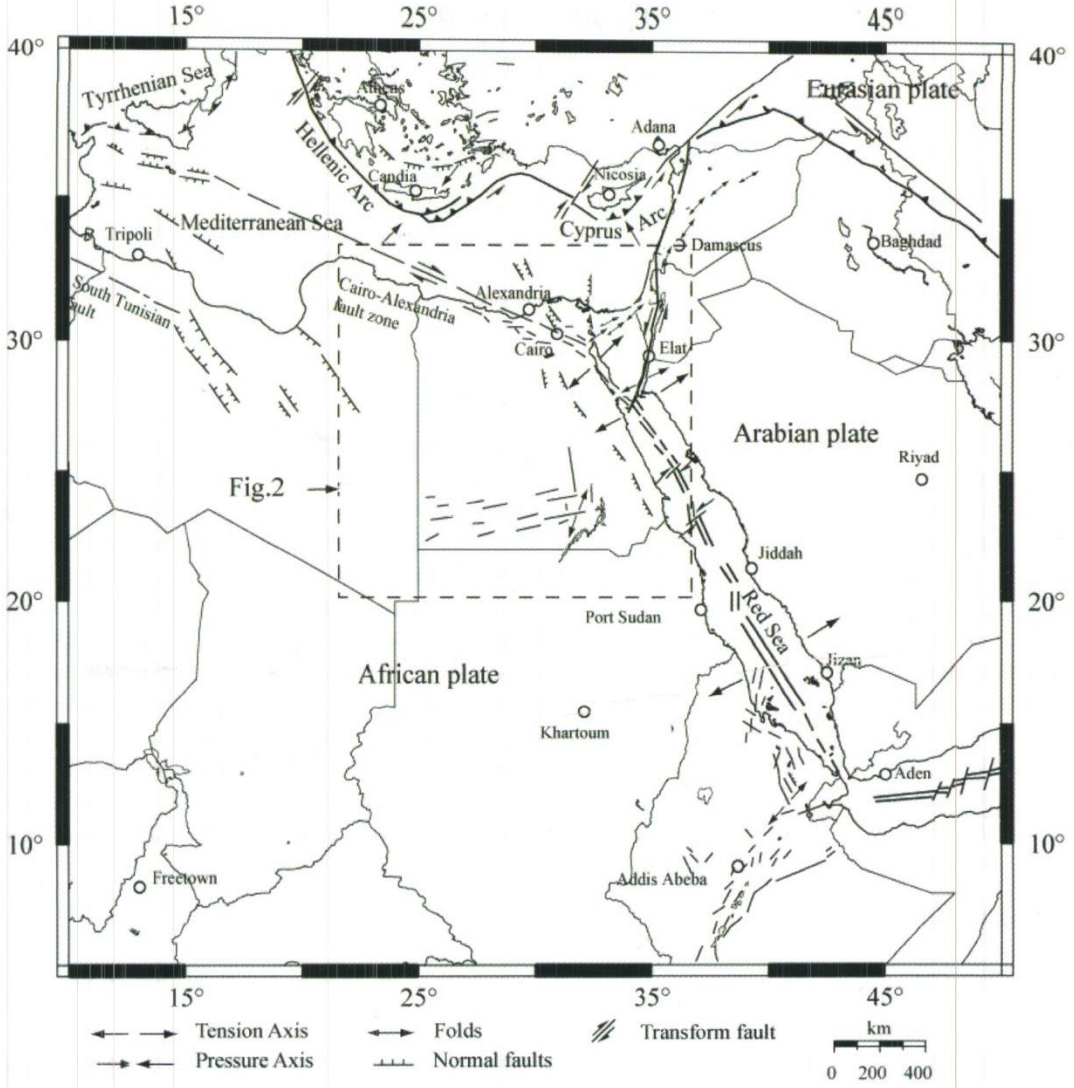

Fig. 1: Regional geodynamic setting of the northeast Africa (modified after Mahmoud, 2003). Study area is shown in dotted rectangle.

down and at that time the direction of extension along the gulf was NE-SW (Angelier 1985, Bosworth and Taviani 1996). With the end of Miocene, the motion shifted from Gulf of Suez to Aqaba-Dead Sea fault system resulting E-W extension along the Gulf of Suez (Steckler and ten Brink 1986; Le Pichon and Gaulier 1988; Lyberis 1988; Steckler et al. 1988; Girdler 1991; Jolivet and Faccenn 2000). The excellent record of early stages of rifting in the Gulf of Suez has been well documented from the geological outcrops, oil wells, geophysical and seismic data of the rift. Morphology of the rift shows intense extension, uplift, and subsidence occurred in the past. Although very low rates of tectonic subsidence and extension (~1 mm/yr) can be observed, at the present Gulf of Suez is best classified as an abandoned or failed rift basin (Moretti and Colletta 1987; Steckler et al. 1988; Patton et al. 1994; Moustafa 1996; Steckler et al. 1998). The low rate of extension and subsidence, however, is believed to be associated with small-scale mantle convection currents below the gulf (Steckler 1985; Steckler et al. 1988).

Various attempts have been put toward producing reliable models for the origin of stress field in the gulf (Steckler 1985; Steckler and ten Brink 1986; Joffe and Garfunkel 1987; Colletta et al. 1988; Garfunkel 1988; Le Pichon and Gaulier 1988; Lyberis 1988; Steckler et al. 1988; 1998; Badawy and Horv´ath 1999c; Badawy 2005; Mahmoud et al. 2005; Taha and Miguel 2008). The main differences among these models are the controlling factors for the geodynamic origin of the rift basin. The factors, either the present-day stress field is originated due to the Gulf of Suez rift itself or due to the

influence of nearby tectonic boundaries, is under question. Therefore, it seems useful to reconstruct the tectonic stress field of the whole northeast Africa and the stress field of the Gulf of Suez and develop a model for the geodynamic origin of Suez rift system.

GEOTECTONIC SETTING

Northeast Africa forms the northernmost extension of the East African Rift System and is considered one of the geodynamically active regions in the Earth. The Red Sea, Gulf of Suez, Gulf of Aqaba, and Dead Sea transform are the most prominent tectonic features in the region (Fig. 2). The main reason of tectonic motion is the stress exerted through northward movement of African and Arabian Plates. Earthquake focal mechanisms near tectonic boundaries of these plates show normal and strike-slip type motion, which support the divergence of these plates (McKenzie, 1972; Huang and Solomon, 1987; Badawy and Horv´ath 1999b; Mahmoud, 2003; Badawy 2005; Hussein et al. 2006; Abdel-Rahman et al. 2009) (Fig. 3). A variety of geological structures in northeast Africa are: (1) NW-SE trending faults parallel to the Red Sea-Gulf of Suez, (2) N-S and NE-SW trending faults parallel to the Gulf of Aqaba and Dead Sea transform (3) E-W trending faults of the eastern Mediterranean (Kebeasy 1990) (Fig. 2). Movement of tectonic plates controls all of these geological structures. Tectonic features of the region are summarized below:

Red Sea rift

The Red Sea rift, which is an about 2000 km long NNW-SSE trending depression, forms a broad zone of active deformation between African and Arabian Plates. It is accompanied by high seismic activity, and is expressed by numerous fractures and normal faults. Seismicity is concentrated along the axial trough which is an area of active spreading and normal faulting associated with African-Arabian Plate extension (Huang and Solomon 1987; Ghebreab 1998; Dwivedi and Hayashi 2009).

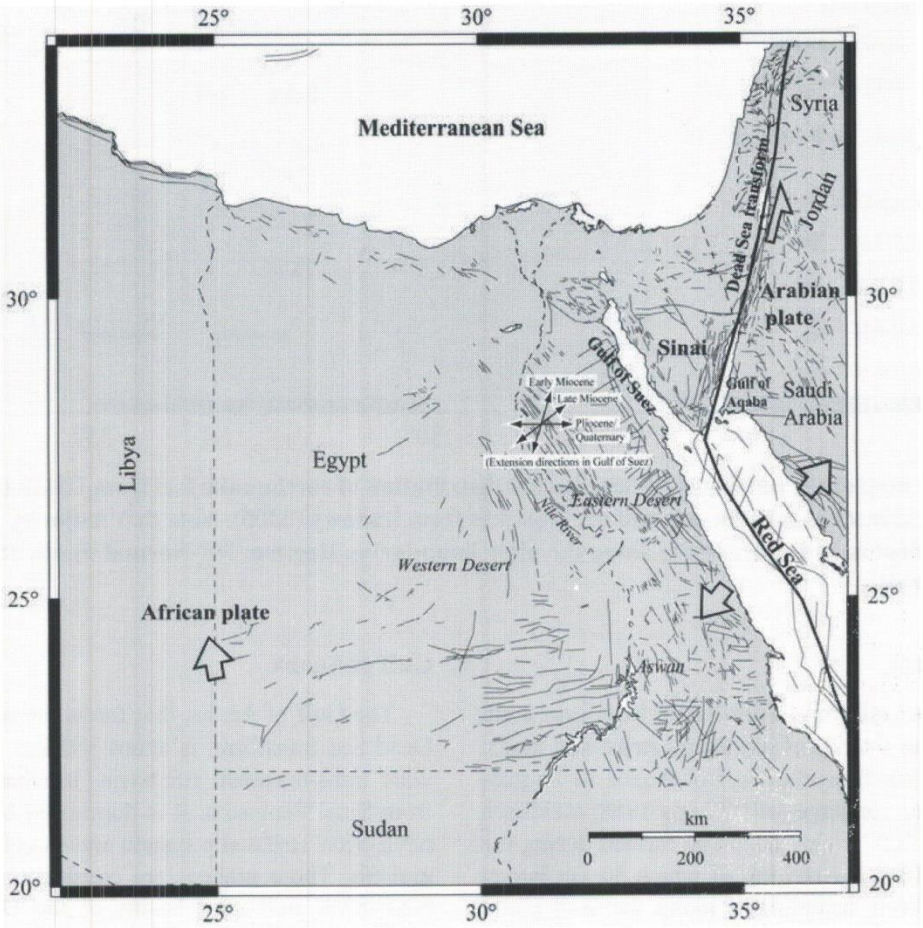

Fig. 2: Tectonic map of northeast Africa showing the location of rifts and faults (thin lines). Thick black line represents African-Arabian plate boundary and thick arrows indicate direction of plate movement. Three phases of extension direction in the Suez rift taken from Lyberis (1988) and Favre and Stampfli (1992).

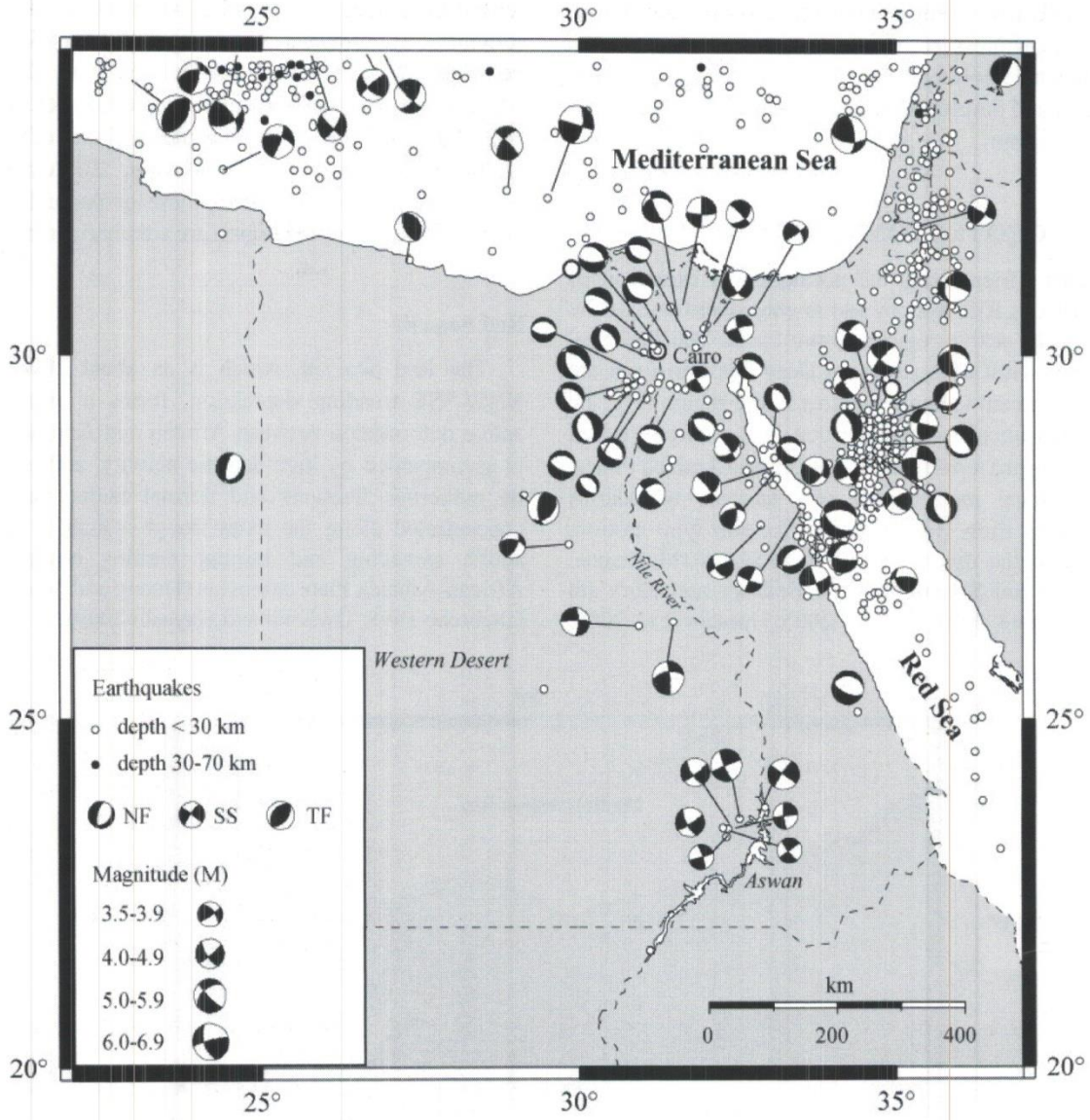

Fig. 3: Seismicity map of the northeast Africa. Spatial distribution of earthquake foci from USGS (http://earthquake.usgs.gov/) and focal mechanisms for selected earthquakes from Badawy (2005). Note that majority of the earthquakes occur at shallow depths and concentrate along the plate boundaries. Regime: NF-Normal Fault, SS-Strike-Slip Fault and TF-Thrust Fault.

Dead Sea transform

The Dead Sea transform is a left lateral transform fault, which is broken into a series of left lateral strike-slip faults, extends over 450 km from the Gulf of Aqaba to Zagros-Taurus area of plate convergence (Lyberis 1988; Heidbach and Ben-Avraham 2007). This fault was formed during the past ~5 Ma and offset is ~105 km of which 30 km lateral displacement has been accumulated along the fault (Joffe and Garfunkel 1987). Dead Sea transform kinematics for the last ~ 5 Ma states that the system had an average slip rate of ~ 7 mm/yr (Westaway 1994).

Gulf of Aqaba

The Gulf of Aqaba, that forms the southernmost part of Dead Sea transform, is about 180 km long and 30-40 km wide trans-tensional rift basin. It separates Arabian Plate from Sinai Peninsula. It is dominated by numerous N-S to NNE-SSW strike-slip system and en-echelon rhomb shaped grabens. These grabens are considered as a succession of NNE-SSW pull-apart basins of the Dead Sea transform (Garfunkel 1988). Field observations show two-stage motion in the Gulf of Aqaba: NE-SW strike-slip motion during the Late Miocene and E-W extension during the Plio-

Quaternary (Lyberis 1988). E-W extension produced N-S trending narrow grabens in the eastern Sinai by extensive normal faulting.

Sinai which lies between the Gulf of Suez and the Gulf of Aqaba, is a part of African (Nubian) Plate and is characterized by strike-slip regime with a number of inter plate seismicity (Badawy and Horv´ath 1999a; Badawy 2001; Badawy 2005; Abdel-Rahman et al. 2009). It is also being treated as separate subplate of Africa (Badawy and Horv´ath 1999a; 1999b; Salamon et al. 2003; Badawy 2005; Mahmoud et al. 2005).

Gulf of Suez

The Gulf of Suez is about 300 km long and 60-80 km wide NW striking slightly arcuate basin that joins the Red Sea across the Gulf of Aqaba rift. As confirmed by numerous drillings, Gulf of Suez is floored by continental crust (Joffe and Garfunkel 1987). Structure of the basin is characterized by numerous normal faults, tilted blocks and asymmetric grabens. Grabens are subdivided by NNE-SSW to NE-SW fault zone basins. Northern and southern basins are characterized by westward tilted blocks while central zone is characterized by eastward tilted blocks (Colletta et al. 1988; Lyberis 1988). Fault pattern shows two major trends: a longitudinal set parallel to the rift axis and transverse set with N-S to NNE-SSW trend, which produced a zig-zag pattern and rhombic-shaped blocks (Fig. 2). Geologic and tectonic history show Suez rift was active for a long time from the Oligocene to Early Miocene. It was characterized by extensional tectonics with large deformation rate, uplift and subsidence in the past (Steckler 1985; Moretti and Colletta 1987; Omar et al. 1989; Steckler et al. 1998). In the Early Miocene, extension was NNE-SSW, which was oblique to the rift, while in the Middle to Late Miocene extension changed to NE-SW (Lyberis 1988). Since the end of Miocene motion shifted progressively from Suez rift to the Aqaba fault system i.e. from NE-SW into E-W direction. This change in direction is believed to be associated with Dead Sea transform tectonics (Lyberis 1988). Observations indicate significant differences in orientation and magnitude of extension between the northern and southern parts of the Suez rift. There is continuing regional uplift and low rates of extension and subsidence mostly in the southern part of the gulf (Steckler 1985; Steckler et al. 1988; Patton et al. 1994; Bosworth and Taviani 1996). The northern part of the gulf has undergone only about 10-15 km of extension, while the southern part has experienced 30-35 km of extension. As a result, northern part of the gulf has fewer tilted fault blocks (Colletta et al. 1988; Patton et al. 1994). This has also been revealed by the distribution of earthquakes in the region. Apart from few evidence of seismicity in its northern and central parts, Gulf of Suez shows the present-day tectonic activity mostly concentrated along the southern part of the rift (Daggett et al. 1986; Kebeasy 1990; Badawy 1999b; Salamon et al. 2003; Hussein et al. 2006; Abdel-Rahman et al. 2009; Dwivedi and Hayashi 2011), which has been attributed to the effect of Dead Sea transform tectonics.

PRESENT DAY STRESS FIELD AND CRUSTAL DEFORMATION

World stress map (WSM)

World Stress Map project provides extensive data set of present-day stress field in northeast Africa (Zoback 1992; Heidbach et al. 2008; Heidbach et al. 2010) (Fig.4a). Various type of stress indicators are used to determine the tectonic stress orientation, such as: focal mechanisms, borehole breakouts and drilling-induced fractures, in-situ stress measurements (overcoring, hydraulic fracturing, borehole slotter) and geologic data (fault slip analysis and volcanic vent alignments). Northeast Africa represents a region of complicated contemporaneous stress pattern and considerably more heterogeneous than in the stable areas of Eurasian Plate (Badawy and Hovarth 1999a; Heidbach et al. 2010) (Fig.4a). WSM show that most of these stresses are concentrated along the plate boundaries. Present-day σ_{Hmax} in northeast Africa mostly trend NW-SE to N-S. Most of the σ_{Hmax} are in the normal fault regimes implying that σ_{Hmax} approximates σ_2 and extension (σ_{hmin}) is perpendicular to σ_{Hmax}.

The most characteristic feature of stress in the region is a gradual rotation of σ_{Hmax} in space along the margins of African and Arabian Plates. Particularly, near the Dead Sea transform, σ_{Hmax} rotates from N-S to NNW-SSE direction. On the other hand, along the southwestern margin of Arabian Plate, from Saudi Arabia, Jordan to southern Syria, σ_{Hmax} changes from NE-SW to E-W. These orientations show obliquity to Dead Sea transform. In contrast, in the Gulf of Suez σ_{Hmax} are not uniformly oriented. Here, σ_{Hmax} trend NE-SW in the northern part, and ENE-WSW to E-W in the southern part. From southern part of the Gulf of Suez to Eastern Desert, gradually changes from NW-SE to WNW-ESE. In Western Desert, σ_{Hmax} takes NW-SE direction and rotates towards southern Egypt, and particularly in Aswan area stress becomes almost E-W. Farther north, at the northern end of the Gulf of Suez to Egyptian coastal area, σ_{Hmax} takes NW-SE to NNW-SSE orientation. In overall, present-day stress pattern for the northeast Africa as revealed by WSM, clearly shows the interplate σ_{Hmax} pattern is nearly in the direction of African and Arabian Plate motions while most of the rotation of stress axis arises in the area of plate

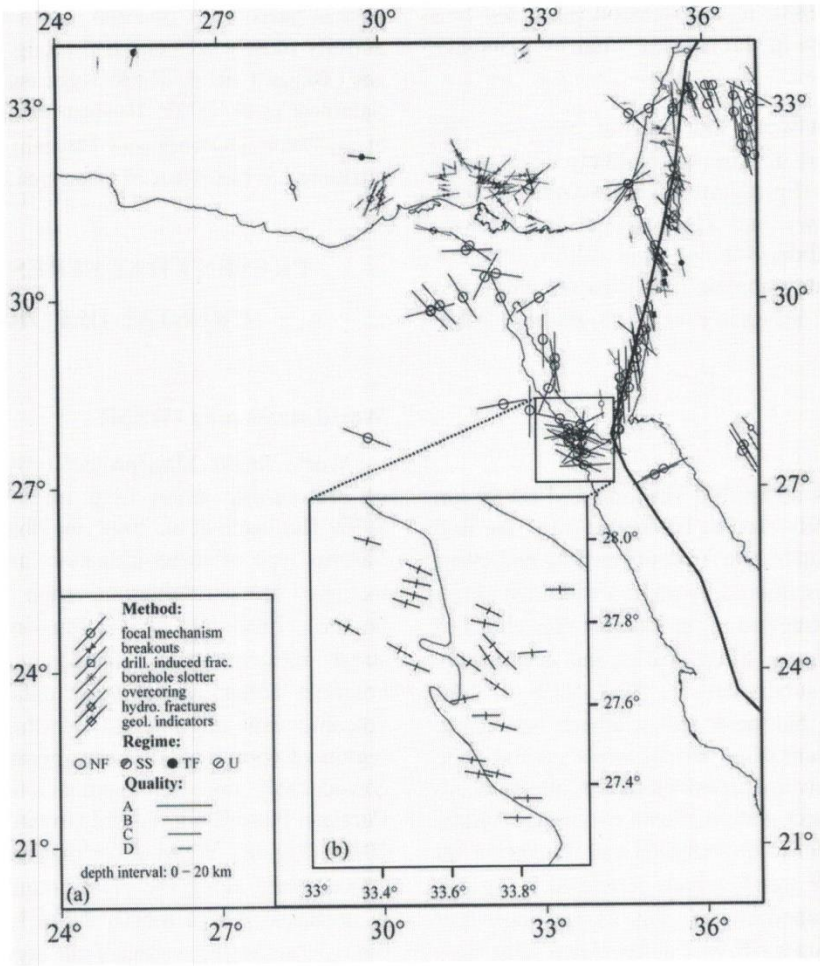

Fig. 4: Observed maximum horizontal compressive stress (σ_{Hmax}) of the northeast Africa, from (a) World Stress Map (WSM), Focal Mechanism Solution (FMS) of earthquakes, in-situ stress measurements and geological stress information (modified after Heidbach et al., 2008; Badawy and Hovarth, 1999a) (b) borehole breakouts data (after Badawy, 2001). Long axis represents σ_{Hmax} and short axis represents σ_{hmin}.

boundaries.

Borehole breakouts

Borehole breakouts are in-situ stress measurements used to determine the direction and magnitude of the local tectonic stress. Such measurements provide shallow crustal stress information that are relatively important in aseismic regions. Borehole breakouts generally illustrate a depth interval intermediate between focal mechanisms and other in-situ stress measurements and geological stress indicators (Zheng et al. 1989; Zoback 1992). In a vertical well penetrating an isotropic rock column, borehole breakouts will form in the direction of minimum horizontal stress (σ_{hmin}) (Zheng et al. 1989). Therefore, the direction perpendicular to the borehole elongation, which results from the breakouts, will indicate the direction of maximum horizontal stress (σ_{Hmax}) (Aadnoy 1990). During last three decades an intensive hydrocarbon exploratory drilling has been carried out in northeast Africa (Strecker and Bosworth 1991; Bosworth et al. 1992; Bosworth and Taviani 1996; Bosworth and Strecker 1997; Badawy 2001; Bosworth 2003), and most of the exploratory drilling wells are located in the Gulf of Suez region (Fig.4b). These studies have confirmed that over large areas of northeast Africa, least horizontal stress (σ_{hmin}) is aligned NE-SW to NW-SE. Along the Red Sea-Gulf of Suez margin, σ_{hmin} remains N-S to NE-SW. In the southern part of the Gulf of Suez, σ_{Hmax} trend WNW-ESE to E-W. In the southern part of Arabian Plate, σ_{hmin} switches to approximately NE-SW; and to the south of eastern Mediterranean, σ_{hmin} rotates slightly according to the geometry of the individual arcs and thrust fronts (Strecker and Bosworth 1991; Bosworth and Taviani 1996).

Seismicity and earthquake focal mechanisms

Earthquake focal mechanisms give information of crustal

stress that is originated at different depths. As the main earthquake activity takes place along recent active faults or plate boundaries, interpretation of earthquakes is important in describing the tectonics of any region. Earthquake focal mechanisms serve as an indicator of regional stress orientations, which do not deviate strongly from the true or actual stress orientations. It is already accepted that the compression (P), tension (T) and intermediate (B) axes obtained from earthquake focal mechanisms correspond to maximum (σ_1), minimum (σ_3) and intermediate (σ_2) principal stress directions respectively (Zoback and Zoback 1980; Gephart and Forsyth 1984).

The combinations of P and T axes are good indicators of the regional σ_{Hmax} and σ_{hmin} directions for the northest Africa (Badawy and Horv´ath 1999a; Badawy 2001 2005; Mahmoud 2003) (Fig. 5). The distribution of P and T axes, however, indicate that the mean regional direction of maximum shortening is less well-constrained than the direction of maximum elongation in this area (Badawy 2001). The spatial distribution of earthquakes clearly reflects the associated deformation pattern in the northeast Africa (Fig. 3). In the northern Red Sea, focal mechanisms for a few earthquake events indicate normal faulting with planes trending approximately NW-SE, which characterizes

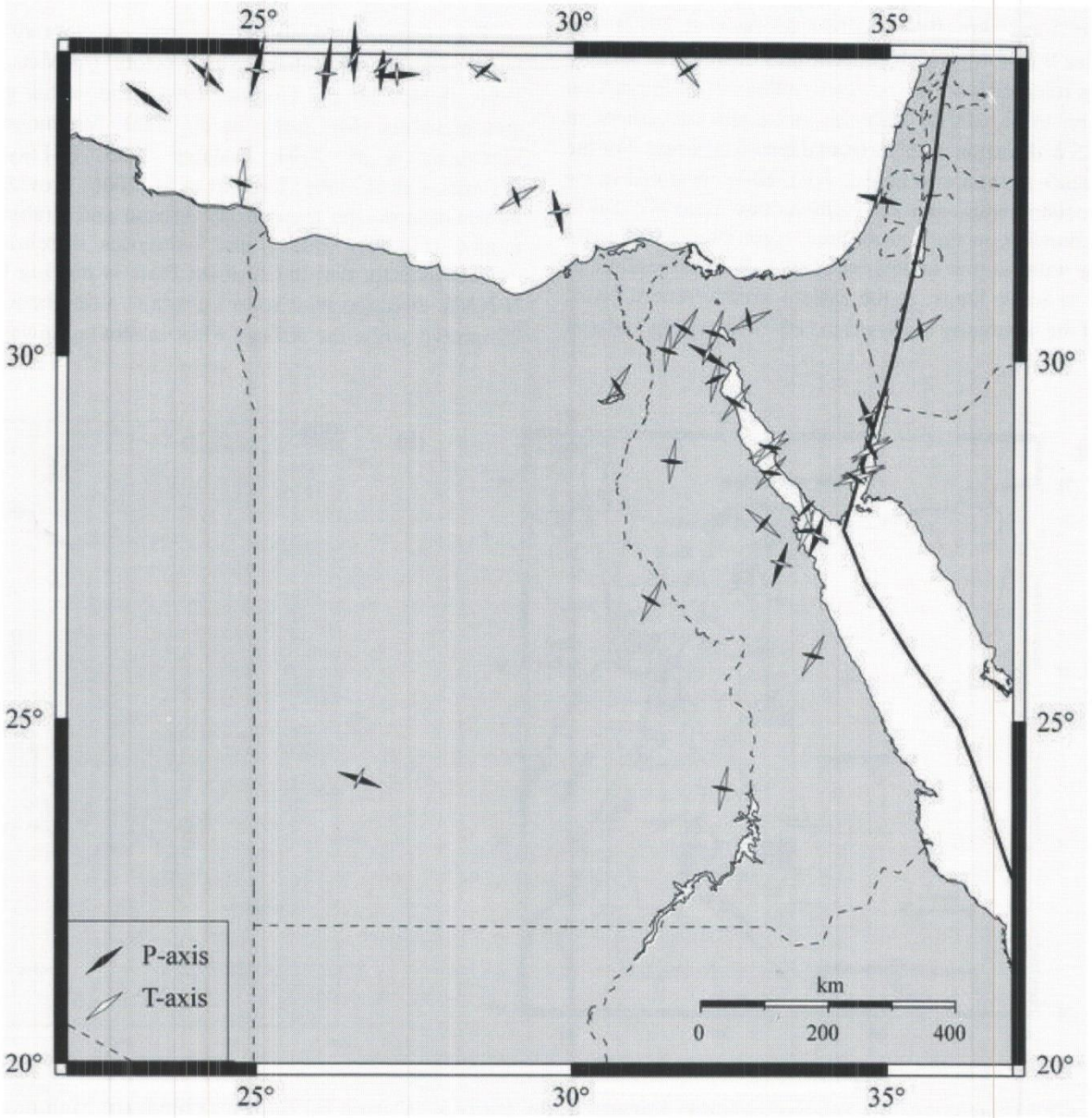

Fig. 5. Stress indicators (P and T axes orientations) from earthquake focal mechanisms in the northeast Africa (after Mahmoud 2003). P-axis: compression, T-axis: tension.

a tensional stress field. Seismic activity in the Gulf of Suez is relatively higher in the southern part which decreases gradually toward north. Focal mechanisms are mostly dominated by oblique normal faulting with left lateral strike-slip components on NW trending fault planes. The presence of faults trending NW-SE that parallel the trend of the gulf are also supported by field observations (Fig. 2). Tensional stress, which is perpendicular to the gulf, is more horizontal and trends NE-SW in the Gulf of Suez. In the Gulf of Aqaba, where numerous moderate earthquakes have been reported, confirms normal type of faulting. For the Gulf of Suez most earthquakes occur at the depths between 10 and 16 km and for the Gulf of Aqaba earthquakes occur between the depths of 5 to 15 km (Badawy 2001; Morsy et al. 2012). The Dead Sea transform which concentrates most of the seismic moment released from the African-Arabian Plate interaction (Salamon et al. 2003), indicates strike-slip movement in NNE-SSW direction with horizontal tensional stress. For the earthquakes in the Cairo region, NNE-SSW tensional stress are associated with some active faults that trend NW-SE to E-W. Likewise, in the Aswan area, right lateral strike-slip faulting with normal component and E-W compression, is related to active faults. In the eastern Mediterranean coast, most of the seismicity is related to NW-SE trending faults of Syrian Arc system. On the other hand, earthquake activity within the area of Egyptian coastal line from northern Nile Delta to the border with Libya is characterized by moderate to large but scattered earthquakes, and does not clarify any trend. In general, focal mechanisms of moderate to large earthquakes affecting the whole northeast African territory show NNE-SSW tensional and WNW-ESE compressional stress axes. The Red Sea, Gulf of Suez, Sinai and Gulf of Aqaba are mainly affected by a tensional stress axis with NE-SW to NNE-SSW trend.

Crustal deformation derived from GPS data

Plate tectonic models derived from sea-floor spreading, fault systems, earthquake slip vectors (DeMets et al., 1990, 1994; Chu and Gordon, 1998), and spatial geodetic measurements (McClusky et al. 2000; Mahmoud 2003; McClusky et al. 2003; Badawy 2005; El-Fiky 2005; Mahmoud et al. 2005; Riguzzi et al. 2006) provide better information on the present-day African and Arabian Plate motion (Fig. 6; Table 1 and references therein). These models indicate that the Arabian Plate is moving towards N-NNW direction relative to Eurasia at a rate between 20-25 mm/yr, while the African Plate is moving towards NW

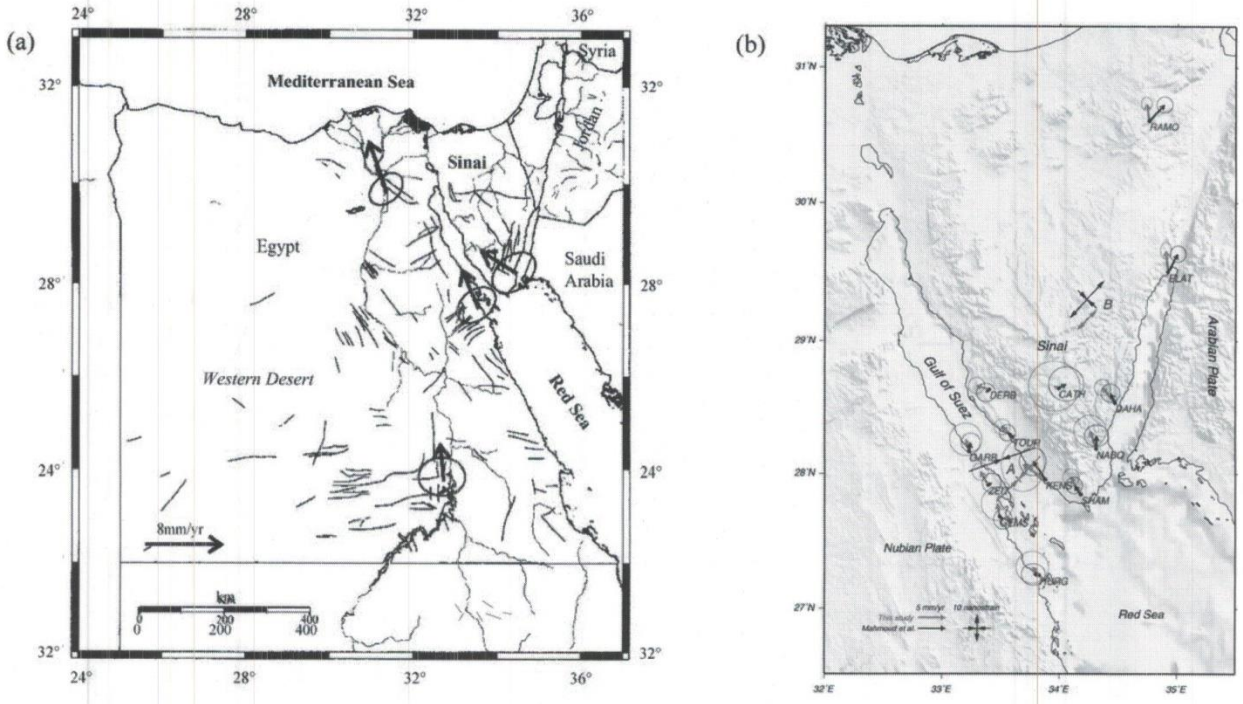

Fig. 6: GPS velocity vectors relative to stable Eurasia in the study area, from (a) Badawy (2005) (b) Mahmoud et al. (2005) and Riguzzi et al. (2006). Gray lines shown in (a) represent active faults. Black and red arrows shown in (b) represent residuals from Mahmoud et al. (2005) and Riguzzi et al. (2006) respectively. Horizontal principal strain axes, black and red bars, from Mahmoud et al. (2005) and Riguzzi et al. (2006), respectively.

at a rate between 6 and 10 mm/yr. The differential motion has been accommodated by the Dead Sea transform with a rate of approximately 10-15 mm/yr and, which is in fact 3/4 of the Africa-Arabia opening (Steckler and ten Brink 1986). Comparing the rate of motion, Dead Sea transform displays a higher rate of movement (8-9 mm/yr) than the Gulf of Suez (0.5-2 mm/yr) and Gulf of Aqaba (5 mm/yr) rifts, which has been confirmed by seismic moment of earthquakes (Badawy and Horv´ath 1999b, Mahmoud 2003; Badawy 2005). Plate motion models suggest that velocities of African and Arabian Plates are slowing down as they move south to north and collide with Eurasia.

MODELING

In this study, by using 2D finite-element program, we model the present-day stress field of the Suez rift. Linear elastic rheology is assumed for the modeling and gravitational force is taken into account assuming that the crust is mechanically isotropic. The detail of mathematical formulation of the 2D plane stress modelling used in this paper is given in Hayashi (2008).

Model domains and material parameters

On the basis of well-recognized tectonic boundaries (Badawy and Horv´ath 1999a; Badawy 2001; Mahmoud 2003; Badawy 2005), the study area (1219 km by 1257 km) is divided into five sub-domains (Fig.7a); (1) African Continental Plate, (2) Mediterranean Sea or African Oceanic Plate, (3) Red Sea rift, (4) Arabian Plate and (5) weak zone. Although there is general agreement for distinct Sinai subplate, we have assumed it as a part of African Plate. Plate boundary is treated as a 'weak zone' that can fail by slip (strike-slip faulting) or separation (normal faulting). Assumption of highly deformable weak zone at the plate boundaries mean to reproduce the relative displacements of African and Arabian Plates. It is assumed that displacements on the weak zone are small with respect to the length and there is no ductile deformation of the material inside this zone. For the purpose of modeling, study area is covered by finite-element mesh containing 1012 triangular elements interconnected with 552 nodal points. Each sub-domain is assigned into elastic and strength parameters (Table 2). The value of material parameters, density (ρ) is adopted from Saleh et al. (2006) and Fischer (2006); Young's modulus (E) of 70 GPa is taken for the crust (Grunthal and Stromeyer 1992; Gölke and Coblentz 1996; Bada et al. 1998; Jarosiński et al. 2006) and 3 GPa for the weak zone (Homberg et al. 1997). Likewise, ideal value of Poisson's ratio (υ), i.e. 0.25, is taken for the overall model, while 0.40 for the weak zone (Jarosiński et al. 2006).

Table 1: Velocities of tectonic plates derived from geologic and geodetic data in the study area.

Tectonic Plate or plate boundaries	Plate velocity range (mm/yr)	Direction of Plate motion	References
African Plate	5 – 12	N to NW	10-12 mm/yr: DeMets et al. (1990) (NUVEL-1A) 4-8 mm/yr: Kahle et al. 1998; Reilinger et al. 2006; Kreemer et al. 2003 < 10mm/yr: Chu and Gordon (1998); McClusky et al. 2000
Arabian Plate	20 – 30	NE to N	20-25 mm/yr: DeMets et al. (1990) (NUVEL-1A); Chu and Gordon (1998) 20-30 mm/yr: McClusky et al. (2000); Reilinger et al. (2006)
Red Sea rift	10 – 20	NE – SW	10-16 mm/yr: Chu and Gordon 1998 17-20 mm/yr: McClusky et al. (2003)
Suez rift	0.5 – 2	NE – SW to E – W	1.6 mm/yr: Joffe and Garfunkel 1987; Bosworth and Taviani (1996); 1.5±0.4 mm/yr: Mahmoud et al. (2005 8-9 mm/yr: Le Pichon and Gaulier 1988; Girdler (1991) 7.5 mm/yr: Westawy 1994
Gulf of Aqaba–Dead Sea Transform	5 – 9	E – W to NE – SW	4-6 mm/yr: Wdowinski et al. (2004); Reilinger et al. 2006; Heidbach and Ben-Avraham (2007)

Table 2: Model parameters.

Model parameters	weak zone	African Plate	Africa Plate (Oceanic)	Arabian Plate	Red Sea Rift	References
Density (kg/m^3)	2400	2750	2850	2750	2850	Saleh et al. (2006); Fischer (2006)
Young's modulus (GPa)	3	70	70	70	70	Grunthal and Stromeyer (1992); Bada et al. (1998); Jarosiński et al. (2006); Gölke and Coblentz (1996)
Poisson's ratio	0.40	0.25	0.25	0.25	0.25	Jarosiński et al. (2006)

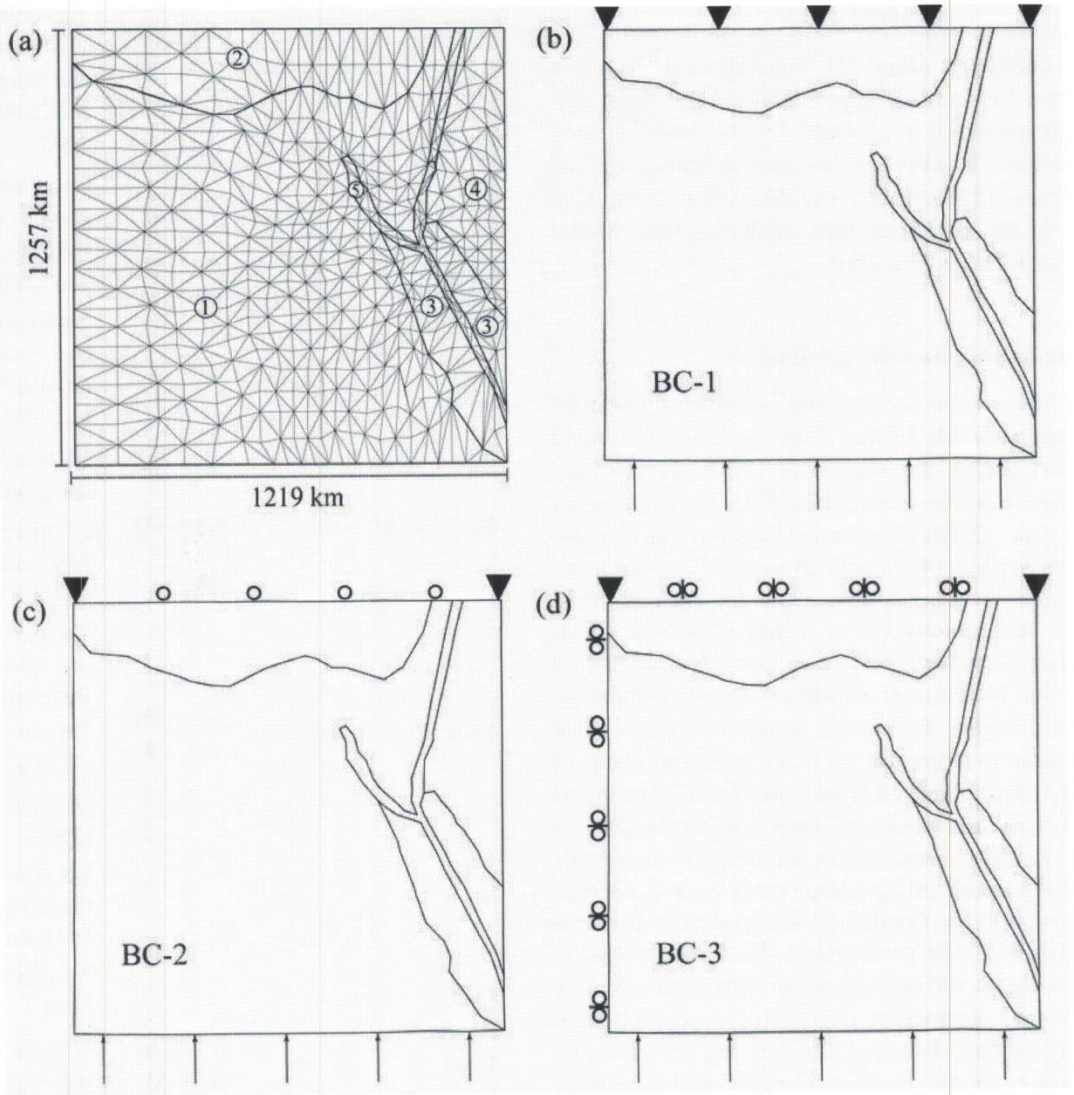

Fig. 7: (a) Finite-element mesh, model geometry, and model domains; 1-African Plate, 2-African Plate (Oceanic), 3-Red Sea rift, 4-Arabian Plate and 5-weak zone. External boundary condition: (b) BC-1: Upper part fix, left and right side fully free (c) BC-2: Upper part free in east-west direction, upper corners fix, left and right sides fully free (d) BC-3: Upper part free in north-south, upper corners fix, left side free in east-west direction, right side fully free. In all models, displacement is imposed from the lower part of model.

Boundary conditions

There is consensus that the African and Arabian Plates are driven by, (a) 'ridge-push force' acting from the Pacific Ocean, southwest Indian Ocean and the Red Sea, (b) 'slab-pull force' and 'collisional force' acting from the north of Africa (Zoback 1992). These forces act as primary or first-order source of homogeneous stress field in northeast Africa, and the relative northward motion of the African and Arabian Plate is the driving force in our model. We use displacements proportional to the velocities of African and Arabian Plates (Table 1). Due to the limitations of FE models, we simply neglect the effect of forces responsible for a second-order stress pattern such as flexural stress of lithospheric bending, gravitational potential energy difference of lithospheric plates, and shear traction induced by mantle convection on the bottom of lithosphere (Zoback 1992).

To determine the most reasonable boundary condition for the present-day stress field and plate motions, various boundary conditions were tested. After a series of tests three types of external boundary conditions BC-1, BC-2, and BC-3 were selected (Figs. 7b,7c,7d). Similarly, after a series of tests, considering the present-day tectonics of the area (Klinger et al. 2000; Reilinger et al. 2006) BC-3 provided the best-fit boundary condition for the northeast Africa in our model. BC-3 was further tested for four cases, in a form of internal boundary conditions, as Case I, Case II, Case III, and Case IV (Table 3, Fig. 8) respectively. This internal boundary condition is, in fact, in accordance to the present-day plate kinematics of the Gulf of Suez and surrounding area (Le Pichon and Gaulier 1988; Lyberis 1988; Steckler et al 1988;) (Table 1). Models were tested respectively for 2, 10, and 20 km crustal depth and for two type of model geometries viz. model with weak zone and model without weak zone (Table 3). For clarity purpose, only representative models are presented in this paper (Fig. 9-13).

Keeping the northward movement of African Plate, we evaluate the relative contribution of Red Sea, Gulf of Suez, Gulf of Aqaba, and Dead Sea transform in our models. Each of these models has been designed to evaluate the influence of (one or combination of) these tectonic forces over the stress field. Case I is adopted to evaluate the effect of boundary conditions representing ridge push force acting from the Red Sea (Fig. 8a), while Case II is used to evaluate the role of Red Sea rift as well as Suez rift (Fig. 8b) in our

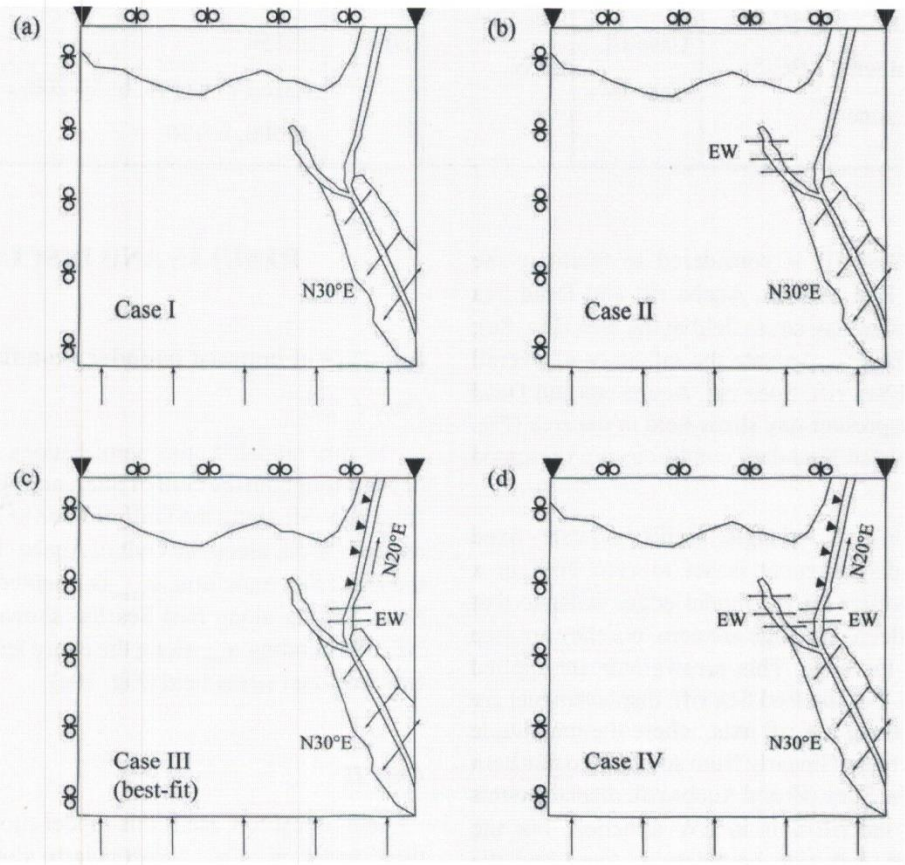

Fig. 8: Internal boundary conditions for the Suez rift model. (a) Case I (b) Case II (c) Case III (d) Case IV. Displacement is imposed from African plate and nearby tectonic boundaries. See Table 3 for further description.

Table 3: Applied displacement and boundary conditions in the finite-element models.*Best fit model conditions

Models	Boundary conditions			Depth (km)	Displacement (m) (a=African plate, b=Red Sea, c=Gulf of Suez, d=Gulf of Aqaba, e=Dead Sea transform)
	External	Internal			
		Cases	Extension direction in the Gulf of Suez		
Model without weak zone	BC-1 BC-2 BC-3*	Case-I Case-II Case-III* Case-IV	NNE-SSW NE-SW E-W*	2*, 10, 20	Case-I: a=10, b=5-20 Case-II: a=10, b=5-20, c=5 *Case-III: a=10, b=5-20, d=5, e=15 Case-IV: a=10, b=5-20, c=5, d=5, e=15
Model with weak zone*					
Model without weak zone	BC-1 BC-2 BC-3	Case-I Case-II Case-III Case-IV	NNE-SSW NE-SW E-W	2, 10, 20	Case-I: a=100, b=50-200 Case-II: a=100, b=50-200, c=50 Case-III: a=100, b=50-200, d=500, e=150 Case-IV: a=100, b=50-200, c=50, d=500, e=150
Model with weak zone					

model. Similarly, Case III is considered to facilitate the contribution of the Red Sea rift, Aqaba rift and Dead Sea transform to the present-day stress field in the area (Fig. 8c); and Case IV is utilized to evaluate the influence of overall contribution of Red Sea rift, Suez rift, Aqaba rift and Dead Sea transform to the present-day stress field in the area (Fig. 8d). Details of the tested boundary conditions are presented in Table 3.

As shown in Fig. 8, triangle marks indicate fixed points, where the displacement is set to zero both in x and y directions. Rollers on the model edges indicate that displacements parallel to the edge are zero, but they are free to move normal to the edge. Thin arrows indicate applied edge displacements. For the Red Sea rift, displacements are imposed at N30°E along the rift axis, where the magnitude of displacement decreases linearly from southern to northern part of the rift. For the Suez rift and Aqaba rift, displacements are imposed along the rift axis in EW direction. For the Dead Sea transform, left side boundary is fixed and the displacements are imposed along right side boundary in a direction parallel to this boundary (N20°E).

RESULTS AND DISCUSSION

Influence of imposed boundary conditions

Case I

In this model, Large perturbations in σ_{Hmax} orientations occur throughout the Gulf of Suez, and changes progressively from NW-SE along the Gulf of Suez to NW-SE in the Sinai, and to NW-SE along the Gulf of Aqaba (Fig. 9a). Throughout the Dead Sea transform, σ_{Hmax} is oriented oblique to the fault zone. Rifting along Red Sea has shown a large number of NE-SW trending σ_{hmin} along the entire length of Red Sea with few tensional stress field (Fig. 10a).

Case II

In contrast to Case I, this model shows some changes in the orientation of σ_{Hmax}, particularly along the Gulf of Suez and the Sinai area, while other parts show almost similar stress pattern as observed in Case I (Fig. 9b). Along the

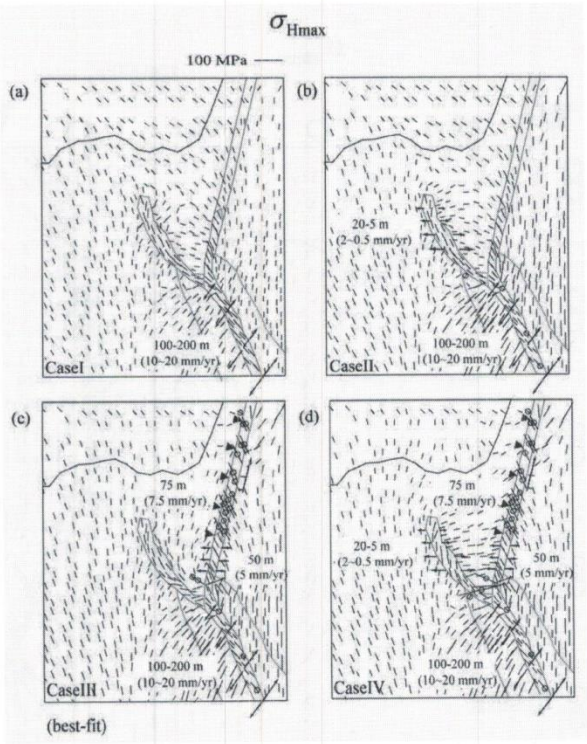

Fig. 9: Calculated maximum horizontal stress (σ_{Hmax}) orientations for the Gulf of Suez rift basin (model with fault zone) at 2 km depth for 10,000 years. (a) Case I (b) Case II (c) Case III (d) Case IV. Small circle shows tensional stress. Case III is the best-fit model.

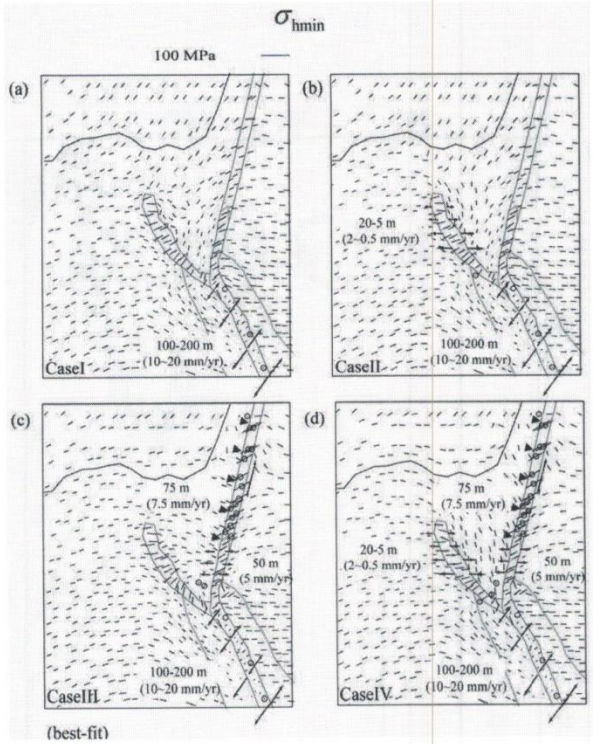

Fig. 10: Calculated minimum horizontal stress (σ_{hmin}) orientations for the Gulf of Suez rift basin (model with fault zone) at 2 km depth for 10,000 years. (a) Case I (b) Case II (c) Case III (d) Case IV. Small circles show tensional stress. Case III is the best-fit model.

entire length of the Gulf of Suez, σ_{Hmax} is oriented N-S while E-W σ_{hmin} directions in the northern and southern part of the gulf with few tensional stress from southern part of the gulf to Red Sea is observed (Fig. 10b). On the other hand, model does not show any tensional stress along the Gulf of Aqaba and Dead Sea transform. In the Sinai area, is oriented almost E-W which rotates to NW-SE along the Dead Sea transform.

Case III

Significant changes in stress field along the Gulf of Suez, Sinai, Gulf of Aqaba, and Dead Sea transform is observed in this model. In the northern part of Gulf of Suez, σ_{Hmax} is oriented NNW-SSE, and in the southern part orientation changes to almost E-W to NE-SW (Fig. 9c). In Sinai, σ_{Hmax} is NNE-SSW to N-S. From southern to central parts of the Dead Sea transform, σ_{Hmax} changes its orientation from NNW-SSE to NW-SE, which is oblique to the fault. Tensional stress is dominant along the central and northern section of the fault. σ_{hmin} along the median zone of Red Sea shows NE-SW direction with few tensional stress (Fig.10c). Moreover, σ_{hmin} vary from NE-SW to E-W along Gulf of Aqaba with few tensional stress in the Sinai area. From the northern end of Gulf of Suez to coastal area of Mediterranean Sea, σ_{Hmax} rotates from N-S to NNE-SSW. σ_{min} are oriented NW-SE in the southern Red Sea, E-W in the northern Red Sea, and almost E-W in the Mediterranean Sea.

Case IV

This model clearly shows the differences in stress pattern from the former model (Fig.10c). Particularly, along the entire length of Gulf of Suez, σ_{Hmax} are oriented N-S with tensional stress in the southern part of the gulf (Fig.9d). The Sinai area shows almost E-W σ_{Hmax}, while E-W σ_{hmin} directions with few tensional stress are observed in the northern and southern part of the Gulf of Suez (Fig.10d). The orientation of σ_{Hmax} along the Dead Sea transform is similar to that observed in the previous model.

Choice of the best-fit model

From all four cases the consequences of imposed boundary condition over the present-day stress field can be seen in the models (Figs. 9 and 10). We describe here the differences between all the four cases and decide the best-fit model. While testing for Case I and Case II, we found similar orientation of σ_{Hmax} near the Gulf of Suez and Gulf of

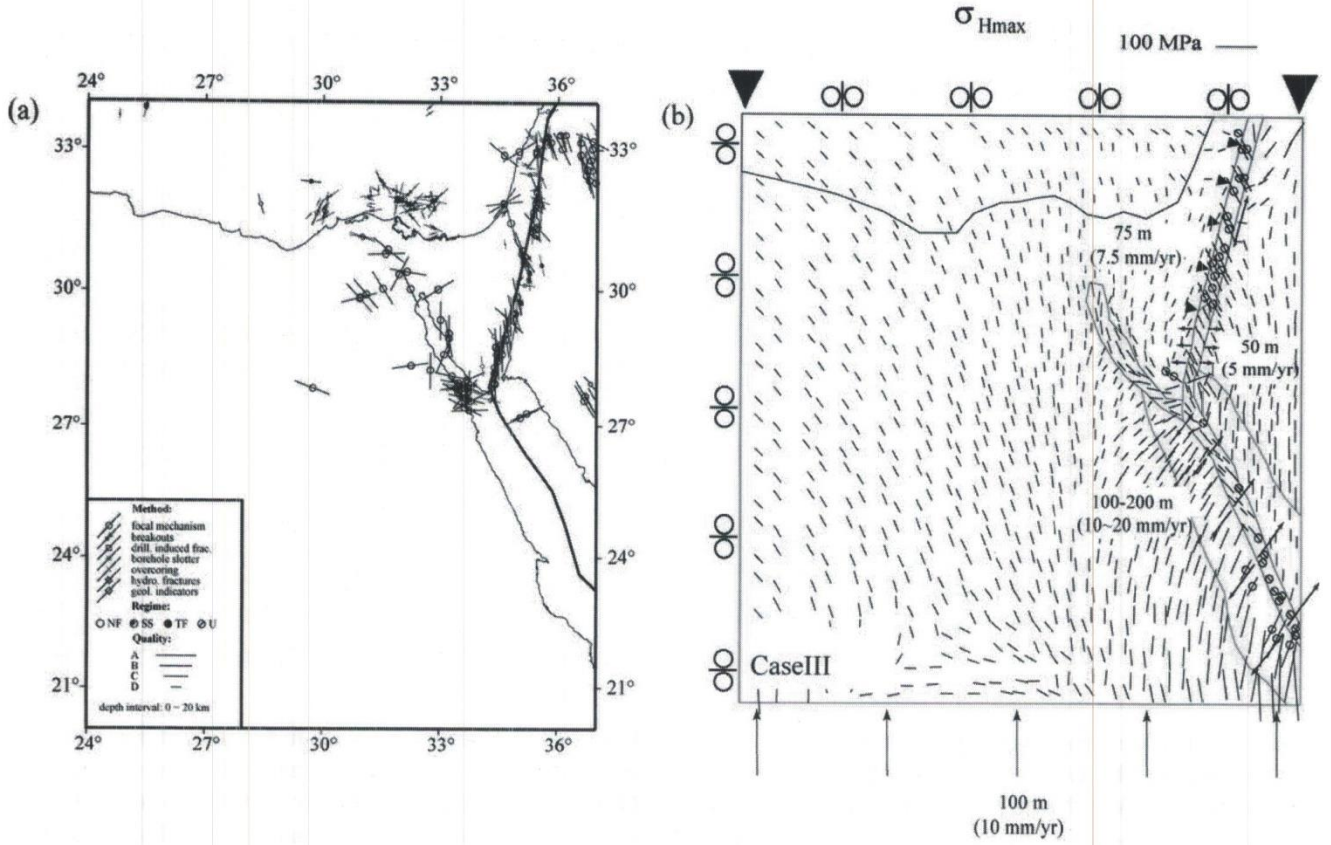

Fig. 11: Comparison of maximum horizontal stress (σ_{Hmax}) field for the northeast Africa from, (a) World Stress Map (WSM), Focal Mechanism Solutions (FMS) of earthquakes, in-situ stress measurements and geological stress information (Heidbach et al. 2008; Badawy and Hovarth 1999a; Badawy 2001) (b) the best-fit model.

Aqaba i.e. NW-SE, which is not consistent with the present-day stress data (compare Fig. 4 and Figs. 9a,b). Similarly, tensional stress field is absent in the Gulf of Aqaba and Dead Sea transform with few present in the southern Gulf of Suez area. These results do not yield satisfactory fit to the observed data (compare Fig.4, Figs. 9a,b and Figs. 10a,b). Likewise, in Case IV, entire length of the Gulf of Suez shows N-S σ_{Hmax} orientations, and few tensional stress with E-W σ_{hmin} orientations, which is not consistent to the observed data (compare Fig. 4, Fig. 9d and Fig. 10d). On the contrary, σ_{Hmax} and σ_{hmin} directions obtained for Case III yield satisfactory fit to the observed stress data (See Fig. 5, Fig. 10c and Fig.11). In this model, NE-SW oriented σ_{hmin} with tensional stress is present along the median zone of Red Sea. Near the Dead Sea transform, σ_{Hmax} are oriented NW-SE, which shows obliquity to the fault zone. Tensional stress is present along the central and northern part of the fault. In addition, throughout the Gulf of Aqaba, orientations of σ_{Hmax} are NW-SE, while σ_{hmin} vary from NW-SE to E-W with few tensional stress. In the Gulf of Suez, orientation of σ_{Hmax} range from N-S to NNE-SSW in northern part, and NW-SE to E-W in the southern part (Fig. 9c). Likewise, σ_{hmin} directions obtained from the model are parallel to some active faults of the African Red Sea margins, Sinai and coastal area of the Gulf of Suez (See Fig. 2 and Fig. 9c). Hence, the boundary condition for Case III seems more plausible and represents the best-fit model in this study.

Observed stress data versus the best-fit model

Regional stress field of the northeast Africa

Study shows the magnitude and pattern of present-day stress field in northeast Africa is dominantly controlled by the tectonic boundary condition due to the movement of African and Arabian Plates. This observation is clearly seen in our models where there is a great deal of variation of σ_{Hmax} and orientations along and across the boundaries of African and Arabian Plates (Fig.9-12). Modeled σ_{Hmax} directions within the continental parts of Nubia and Arabian Plate are compatible with the compressional force acting due to northward movement of African Plate and

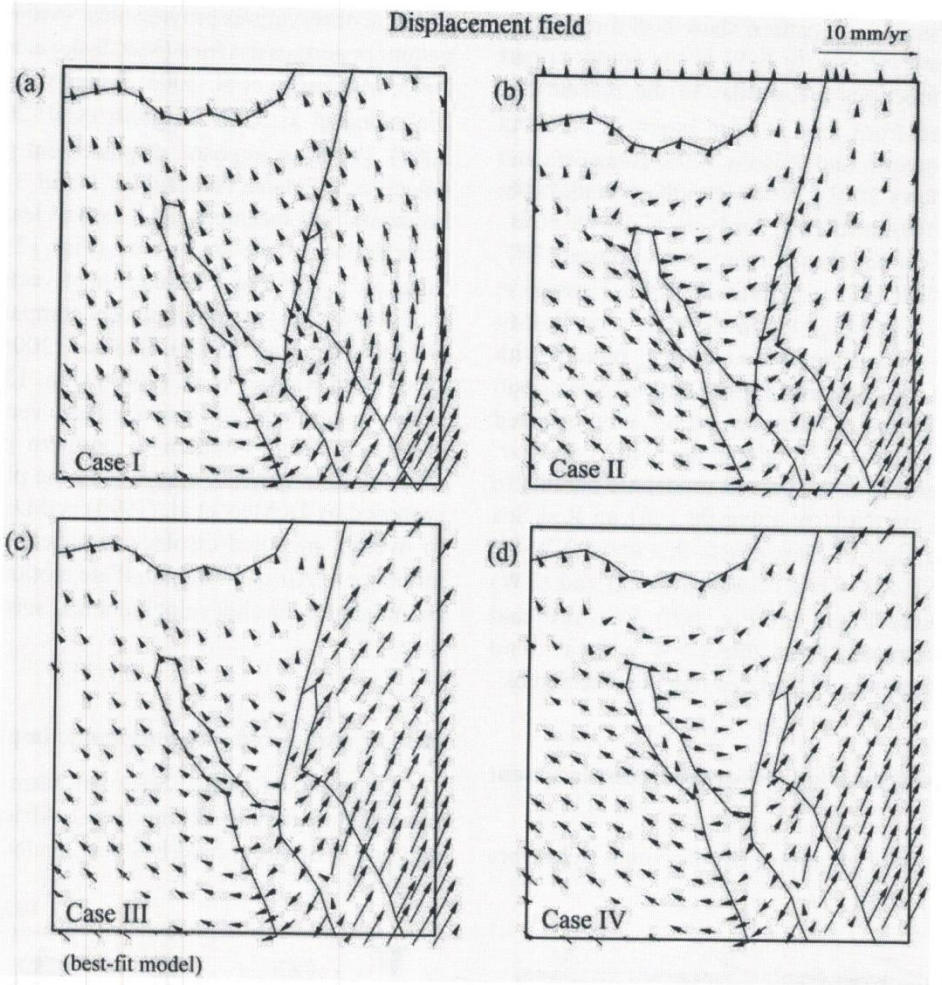

Fig. 12: Calculated displacement field for the northeast Africa, (a) Case I (b) Case II (c) Case III (d) Case IV. Case III is the best-fit model.

northeastward movement of Arabian Plate. On the other hand, σ_{hmin} directions are compatible to the extensional force acting due to divergence of these African and Arabian Plates. For the most part of African Plate, σ_{Hmax} trend NW to NNW, that is compatible to NW African drift direction, and for the Arabian Plate trend NE to N that is compatible to NNW Arabian drift direction (Zoback 1992; DeMets et al. 1990; 1994; McClusky et al. 2000). This result clearly shows the variation of stress field in northeast Africa controlled by the consequence of the African and Arabian Plate motions. It is also obvious that σ_{Hmax} orientations are in the direction parallel to absolute motion of these plates but reflects inhomogeneous stress pattern. The inhomogeneous stress pattern, which has also been confirmed by the studies of earthquake focal mechanisms, borehole breakouts and geological stress information in the area (Badawy 2001; Badawy and Hovarth 1999a; Mahmoud 2003), is attributed to the combined influence of far-field ridge push forces in the Atlantic Ocean, Indian Ocean, and Red Sea basin (Zoback 1992). The inhomogeneous stress pattern recognized in our model, however, is due to the effect of lateral change in crustal strength parameters incorporated in the domains of our models.

Stress field in the Gulf of Suez basin

In the study area, NE-SW oriented σ_{hmin} with few tensional stress along the median zone of Red Sea and Gulf of Aqaba region, correlated with the WSM and seismicity studies (Fig. 3, Fig. 4 and Fig. 5), are considered to be related to their openings (Le Pichon and Gaulier 1988; Steckler et al. 1988). Throughout the Gulf of Aqaba, σ_{Hmax} is NW-SE, while σ_{hmin} vary from NW-SE to E-W. As pointed out by Lyberis (1988), this direction represents the post Miocene extension direction that is oblique to the rift orientation. In case of plate boundaries, NW-SE σ_{Hmax} and NE-SW σ_{hmin} represents the direction of transtensional strike-slip movements. These directions are comparable to the P-axes and T-axes orientations obtained from the FMS of earthquakes and field observations (Lyberis 1988; Badawy 2001) (Fig. 5).

In the Gulf of Suez, σ_{Hmax} pattern show N-S direction in the northern part and NE-SW to E-W in the southern part (Fig. 12). These directions are similar to the present-day stress field obtained from near surface borehole breakout measurements (Bosworth and Taviani 1996; Bosworth and Strecker 1997; Badawy 2001), WSM (Heidbach et al. 2008; Heidbach et al. 2010), structural analysis (Colletta et al., 1988) and FMS of earthquakes (Huang and Solomon 1987; Badawy and Horv´ath 1999a; Mahmoud, 2003; Hussein et al. 2006) (See Fig. 5 and Fig. 12) in the area. Our best-fit model also shows a good correlation of σ_{Hmax} pattern with the principal strain axes obtained for the Gulf of Suez basin by El-Fiky (2005), where maximum strain axes oriented almost NE-SW to nearly E-W along the gulf. Likewise, σ_{hmin} directions obtained for the best-fit model are parallel to some active faults, particularly along the African Red Sea margins, Sinai and Gulf of Suez coasts that show NW-SE (Red Sea trend), NE-SW (Gulf of Aqaba trend) and (EW) (Mediterranean trend) (Fig. 2 and Fig. 10b). Bosworth and Taviani (1996) interpreted these directions as local trend related to Gulf of Aqaba and Dead Sea transform tectonics.

Observed crustal deformation versus Model displacement field

Apart from stress orientations, displacement field from geodetic observations provide clear evidence of deformation pattern in northeast Africa (McClusky et al. 2000; Mahmoud 2003; McClusky et al. 2003; Badawy 2005; El-Fiky 2005; Mahmoud et al. 2005; Riguzzi et al. 2006; Gomez et al. 2007). We have imposed displacement proportional to the velocities of plates (see Tables 1 and 3) and the obtained horizontal displacement field shows clear pattern of crustal deformation in the study area (Fig. 12). Except southern Sinai area, horizontal displacement vectors for the best-fit model (Fig. 12c) are qualitatively comparable to the studies of McClusky et al. (2000), Badawy (2005), Mahmoud et al. (2005) and Riguzzi et al. (2006) (Fig. 13). Modeling result shows magnitude of displacement vectors progressively decreasing from southern to northern part of the model. This trend, in general, agrees with the plate motion models proposed by DeMets et al. (1990) and DeMets et al. (1994). In overall, modeled displacement field clearly reveals the influence of African-Arabian Plate motion for the stress field changes, structural development and seismicity in the study area.

Best-fit model and its geodynamic implications

As discussed earlier, Suez rift basin is geodynamically important region in the northeast Africa, where a source and origin of stress field has been under discussion. WSM,

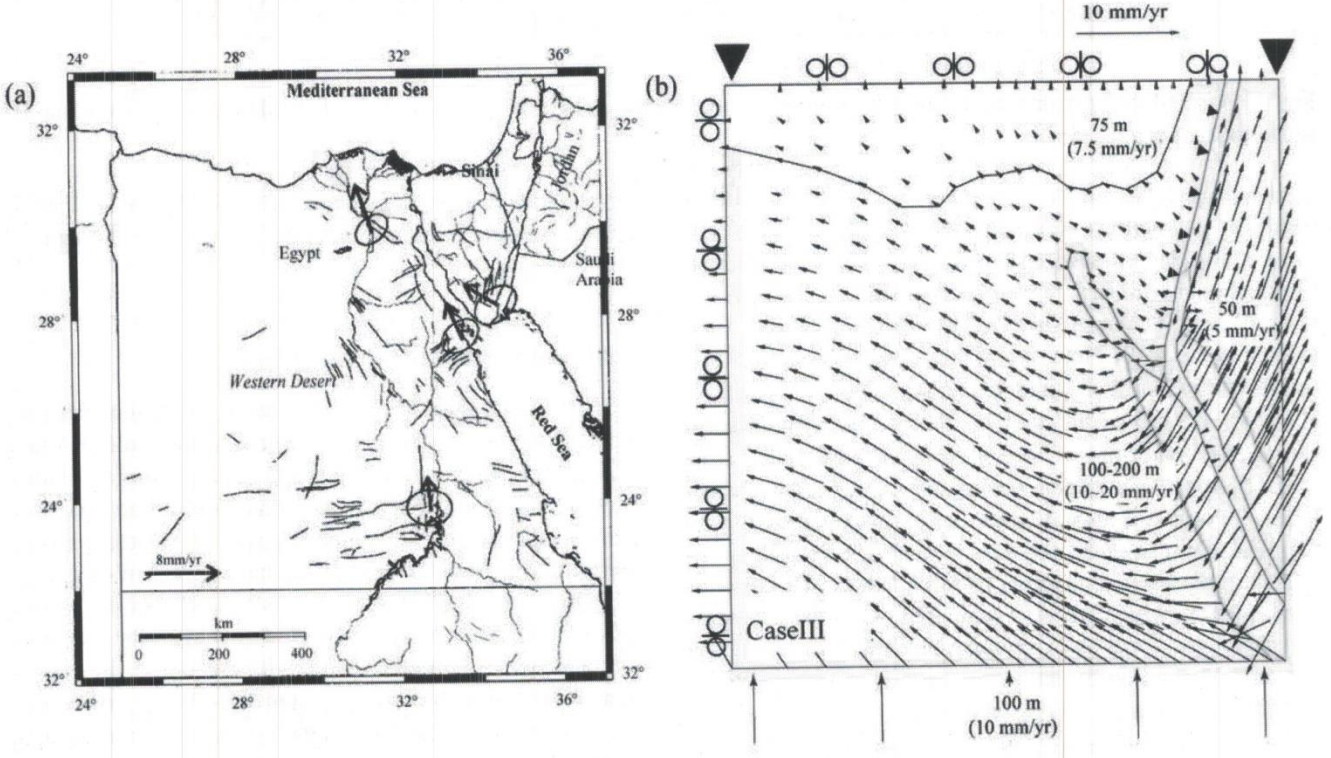

Fig. 13: Comparison of the displacement field for the northeast Africa, from (a) GPS data (Badawy, 2005) (b) best-fit model.

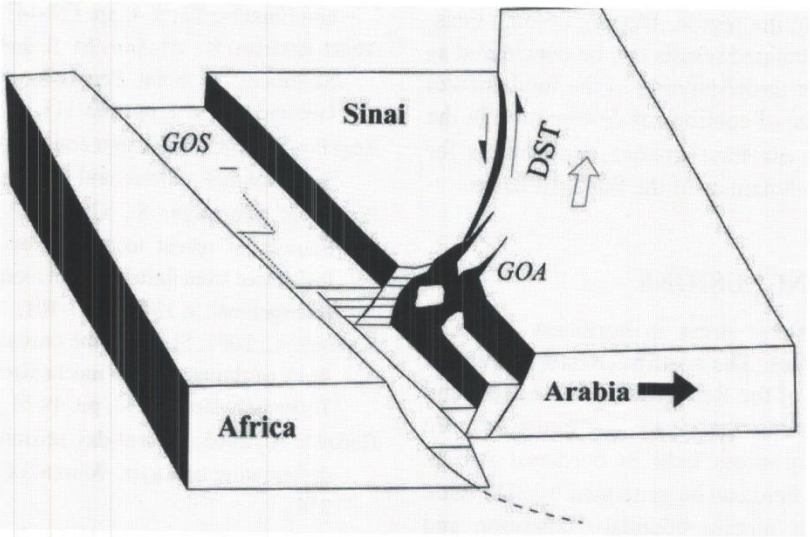

Fig. 14: Proposed model for the present-day tectonics of the Suez rift basin. GOS: Gulf of Suez, GOA: Gulf of Aqaba and DST: Dead Sea Transform.

seismicity, active hydrocarbon exploration, and excellent geological exposures have provided extensive database on the rift. Previous analyses have outlined on a debatable issue of its dynamic history of rifting. This rift has been active since Miocene with periodical uplift, extension and subsidence due to African-Arabian Plate motion (Steckler and ten Brink 1986; Lyberis 1988; Girdler 1991). However, it has been inactive for the last 5 Ma, yet several Plio-Quaternary sedimentary basins can be identified (Steckler et al. 1988; Moretti and Colletta 1987; Patton et al. 1994; Moustafa 1996). Most of the present-day deformation, active faulting and low rate of subsidence in the gulf are believed to be associated with movement along Gulf of Aqaba and Dead Sea transform boundaries (Joffe and Garfunkel 1987; Garfunkel 1988; Lyberis 1988; Steckler et al. 1988; Bosworth and Taviani 1996; Badawy and Horv´ath 1999b; Morsy et al. 2012).

Using 2D plane stress finite-element (FE) method, we modeled the tectonic stress field of Gulf of Suez by taking account of the tectonic loading due to plate motion. We tested the hypothesis, whether the present-day stress field of the Gulf of Suez is induced by Suez rift itself or due to far field stresses by nearby tectonic boundaries viz. Red Sea, Gulf of Aqaba, and Dead Sea transform. We calculated the stress field by taking account of the regional tectonics by imposing extension in the Red Sea, Gulf of Aqaba, Dead Sea transform, and Gulf of Suez in our models. Based on material parameters and varying boundary conditions various models were tested. After series of tests, the best-fit model has been obtained based on the present-day tectonic plate motion, world stress map (WSM) and focal mechanism solution (FMS) of earthquakes in the region. The best-fit model reveals the present-day stress field in the Gulf of Suez is controlled by far field stress generated by the movement along Red Sea, Gulf of Aqaba and Dead Sea transform boundaries. On the basis of modeling results the schematic model for the Suez rift basin is presented (Fig.14) which clearly reveals the present-day tectonics of the region.

MODELING LIMITATIONS

Several methods have been proposed in order to construct a regional stress pattern of the tectonic plates, e.g. averaging of data cluster to obtain a generalized stress field (Muller et al. 1992), statistical smoothing of stress field (Hansen and Mount 1990), linear interpolation of weighted average stress directions (Badawy and Horv´ath 1999a), etc. Finite-element (FE) modeling, adopted in this study, is one of the basic nonetheless widely used tools for the simulation of intraplate and interplate stress field and deformation in the earth crust (Gölke and Coblentz 1996; Lesne et al. 1998; Bird 1999; Petit and Fournier 2005; Dwivedi and Hayashi 2009; Dwivedi and Hayashi 2010; Dwivedi and Hayashi 2011). In the northeast Africa, WSM project (Zoback 1992; Badawy 2001; Badawy 2005; Heidbach et al. 2010) provides an important data set on the first-order pattern of the regional stress field and we use this data for comparison and further verifications with the modeling results. Comparison between the best-fit model and the observed data, however, is not straightforward due to the variation of along strike fault or plate geometry. Observed data from WSM, FMS, and in-situ stress measurements show few and scattered stress indicators for the most part of African and Arabian Plates. Assumption of elastic rheology, on the other hand, does not permit to take account of the thermal effects and related subsidence pattern that might have controlled the deformation and

present-day stress field in the region. Despite of such facts, we emphasize that the obtained results can be considered as a first step towards better understanding of the fundamental nature and dynamic cause of continental deformation in the northeast Africa, which can have greater implications for future studies on the geodynamics of the Suez rift basin.

CONCLUSIONS

The state of present-day stress in northeast Africa is governed by various forces. The northwestward movement of African Plate, rifting of the Red Sea-Gulf of Aqaba, and left lateral movement along the Dead Sea transform, are affecting the present-day stress field in northeast Africa. Study shows such stress field can be generated by 2D elastic plane stress model with precise boundary condition and plate kinematics. When simulated the regional stress field incorporating the present-day tectonic boundary condition, plate boundary forces remarkably constrain the intraplate stress pattern in our model. African and Arabian Plate motion dominantly controls the magnitude and pattern of the first order stress field in the area. Modeled σ_{Hmax} pattern are parallel to the direction of absolute motion of these plates and large perturbations in σ_{Hmax} occur at the plate boundaries. Results of modeling highlight the stress pattern to be consistent with the present-day stress field from WSM, FMS of earthquakes, in-situ stress measurements and geological stress indicators in the northeast Africa. It can be clearly seen that the present-day stress field to be largely controlled by regional plate tectonic stress from collision in the north and spreading in the east and southeast. The best-fit model reveals the coeval influence of Red Sea rift, Gulf of Aqaba rift and Dead Sea transform responsible for the origin and changes of stress field in the Suez rift basin. This suggests that in the present-day tectonics, the Gulf of Suez is geodynamically controlled by far field effect of these tectonic boundaries.

ACKNOWLEDGEMENTS

We would like to acknowledge the Japanese Ministry of Education, Culture, Sports, Science and Technology (Monbukagakusho) for the funding of this research. Anonymous reviewers are thankful for constructive comments, which significantly improved the quality of manuscript. Figures 1, 2, 3 and 5 are generated by Generic Mapping Tool (GMT) (Wessel and Smith 1995).

REFERENCES

Aadnoy, B. S., 1990, Inversion technique to determine the in-situ stress from field fracturing data. Journal of Petroleum Science and Engineering, v. 4, pp. 127-141.

Abdel-Rahman, K., Al-Amri M. S. and Abdel-Moneim, E., 2009, Seismicity of Sinai Peninsula, Egypt. Arabian Journal of Geosciences, v. 2, pp. 103-118.

Angelier, J., 1985, Extension and rifting: the Zeit region, Gulf of Suez. Journal of Structural Geology, v. 7, pp. 605-612.

Bada, G., Cloetingh, S., Gerner, P. and Horv´ath, F., 1998, Sources of recent tectonic stress in the Pannonian region: inferences from finite element modelling. Geophysical Journal International, v. 134, pp. 87-101.

Badawy, A., 2001, Status of the crustal stress in Egypt as inferred from earthquake focal mechanisms and borehole breakouts. Tectonophysics, v. 343, pp. 49-61.

Badawy, A., 2005, Present-day seismicity, stress field and crustal deformation of Egypt. Journal of Seismology, v. 9, pp. 267-276.

Badawy, A. and Horvath, F., 1999a, Recent stress field of the Sinai subplate region. Tectonophysics, v. 304, pp. 385-403.

Badawy, A. and Horvath, F., 1999b, Seismicity of the Sinai subplate region: kinematic implications. Journal of Geodynamics, v. 27, pp. 451-468.

Badawy, A. and Horvath, F., 1999c, The Sinai sub-plate and tectonic evolution of the northern Red Sea region. Journal of Geodynamics, v. 27, pp. 433-450.

Bird, P., 1999, Thin-plate and thin-shell finite-element programs for forward dynamic modeling of plate deformation and faulting. Computer and Geosciences, v. 25, pp. 383-394.

Bosworth, W., 2003, North Africa-Mediterranean Present-day Stress Field Transition: Implications for Fractured Reservoir Production. Extended abstract, American Association of Petroleum Geologists, Hedberg Conference, Algiers, Algeria.

Bosworth, W. and Strecker, M. R., 1997. Stress field changes in the Afro-Arabian rift system during the Miocene to Recent period. Tectonophysics, v. 278, pp. 47-62.

Bosworth, W., Strecker, M. R. and Blisniuk, P. M., 1992, Integration of East African paleo and present-day stress data: Implications for continental stress field dynamics. Journal of Geophysical Research, v. 97, pp. 11851-11865.

Bosworth, W. and Taviani, M., 1996, Late Quaternary reorientation of stress field and extension direction in the southern Gulf of Suez, Egypt: Evidence from uplifted coral terraces, mesoscopic fault arrays and borehole breakouts. Tectonics, v. 15, pp. 791-802.

Chu, D. and Gordon, R. G., 1998, Current plate motions across the Red Sea. Geophysical Journal International, v. 135, pp. 313-328.

Colletta, B. Quellec, P., Letouzey, J. and Moretti, I., 1988, Longitudinal evolution of the Suez rift structure (Egypt). Tectonophysics, v. 153, pp. 221-233.

Daggett, P. H., Morgan, P., Boulos, F. K., Hennin, S. F., El-Sherif, A. A., El-Sayed, A. A., Basta, N. Z. and Melek, Y. S., 1986, Seismicity and active tectonics of the Egyptian Red Sea margin and the northern Red Sea. Tectonophysics, v. 125(4),

pp. 313-324.

DeMets, C., Gordon, R. G., Argus, D. F. and Stein, S., 1990, Current plate motions. Geophysical Journal International, v. 101(2), pp. 425-478.

DeMets, C., Gordon, R. G., Argus, D. F. and Stein, S., 1994, Effect of recent revisions to the geomagnetic reversal time scale on estimates of current plate motions. Geophysical Research Letters, v. 21(20), pp. 2191-2194.

Dwivedi, S. K. and Hayashi, D., 2009, Numerical modeling of the development of southeastern Red Sea continental margin. Earthquake Science, v. 22 (3), pp. 239-249. doi: 10.1007/s11589-009-0239-3.

Dwivedi, S. K. and Hayashi, D., 2010, Modeling the contemporary stress field and deformation pattern of eastern Mediterranean. Journal of Earth Science, v. 21(4), pp. 365-381. doi: 10.1007/s12583-010-0100-6.

Dwivedi, S. K. and Hayashi, D., 2011, Modeling approaches to understand the dynamics of continental deformation: perspective from rifting and collision tectonics. In: Benjamin Veress and Jozsi Szigethy (eds). Horizons in Earth Science Research, Nova Science Publishers, New York, v. 5, pp. 1-80.

Fischer, K. D., 2006, The influence of different rheological parameters on the surface deformation and stress field of the Aegean-Anatolian region. International Journal of Earth Sciences, v. 95, pp. 239-249.

El-Fiky, G., 2005, GPS-derived velocity and crustal strain field in the Suez-Sinai Area, Egypt. Bulletin of Earthquake Research Institute, University of Tokyo, v. 80, pp. 73-86.

Favre, P. and Stampfli, G. M., 1992, From rifting to passive margin: examples of the Red Sea, central Atlantic and Alpine Tethys. Tectonophysics, v. 141, pp. 135-150.

Garfunkel, Z., 1988, Relation between continental rifting and uplifting: evidence from the Suez rift and northern Red Sea. Tectonophysics, v. 150, pp. 33-49.

Gephart, J. and Forsyth, D., 1984, An improved method for determining the regional stress tensor using earthquakes focal mechanism data: an application to San Fernando earthquake sequence. Journal of Geophysical Research, v. 89, pp. 9305-9320.

Ghebreab, W., 1998, Tectonics of the Red Sea region reassessed. Earth Science Reviews, v. 45, pp. 1-44.

Girdler, R. W., 1991, The Afro-Arabian rift system-an overview. Tectonophysics, v. 197, pp. 139-153.

Gölke, M. and Coblentz, D., 1996. Origins of the European regional stress field. Tectonophysics, v. 266, pp. 11-24.

Gomez, F., Karam, G., Khawlie, M., McClusky, S., Vernant, P., Reilinger, R., Jaafar, R., Tabet, C., Khair, K. and Barazangi, M., 2007, Global Positioning System measurements of strain accumulation and slip transfer through the restraining bend along the Dead Sea fault system in Lebanon. Geophysical Journal International, v. 168(3), pp. 1021-1028.

Grunthal, G. and Stromeyer, D., 1992, The recent crustal stress field in Central Europe: trajectories and finite element modeling. Journal of Geophysical Research, v. 97, pp. 11805-11820.

Guiraud, R. and Bosworth, W., 1999, Phanerozoic geodynamic evolution of northeastern Africa and the northwestern Arabian platform. Tectonophysics, v. 315, pp. 73-108.

Hansen, K. M. and Mount, V.S., 1990, Smoothing and extrapolation of crustal stress orientation measurements. Journal of Geophysical Research, v. 95, pp. 1155-1165.

Hayashi, D., 2008, Theoretical basis of FE simulation software package. Bulletin of Faculty of Science University of the Ryukyus, v. 85, pp. 81-95.

Heidbach, O. and Ben-Avraham, Z., 2007, Stress evolution and seismic hazard of the Dead Sea fault system. Earth and Planetary Science Letters, v. 257(1-2), pp. 299-312.

Heidbach, O., Tingay, M., Barth, A., Reinecker, J., Kurfeß, D. and Müller, B., 2008, The world stress map database release 2008, doi: 10.1594/GFZ. WSM. Rel2008.

Heidbach, O., Tingay, M., Barth, A., Reinecker, J., Kurfeß, D. and Müller, B., 2010, Global crustal stress pattern based on the World Stress Map database release 2008. Tectonophysics, v. 482(1), pp. 3-15.

Homberg, C., Hu, J. C., Angelier, J., Bergerat, F. and Lacombe, O., 1997, Characterization of stress perturbations near major fault zones: insights from 2-D distinct-element numerical modelling and field studies (Jura mountains). Journal of structural geology, v. 19(5), pp. 703-718.

Huang, P. Y. and Solomon, S. C., 1987, Centroid depths and mechanisms of mid-oceanic ridge earthquakes in the Indian Ocean, Gulf of Aden and Red Sea. Journal of Geophysical Research, v. 92, pp. 1361-1383.

Hussein, H. M., Marzouk, I., Moustafa, A. R. and Hurukawa, N., 2006, Preliminary seismicity and focal mechanisms in the southern Gulf of Suez: August 1994 through December 1997. Journal of African Earth Sciences, v. 45(1), pp. 48-60.

Jarosiński, M., Beekman, F., Bada, G. and Cloetingh, S. A. P. L., 2006, Redistribution of recent collision push and ridge push in Central Europe: insights from FEM modelling. Geophysical Journal International, v. 167(2), pp. 860-880.

Joffe, S. and Garfunkel, Z., 1987, Plate kinematics of the circum Red Sea- a re-evaluation. Tectonophysics, v. 141, pp. 5-22.

Kahle, H. G., Straub, C., Reilinger, R., McClusky, S., King, R., Hurst, K., Veis, G., Kanstens, K. and Cross, P., 1998, The strain rate field in the eastern Mediterranean region, estimated by repeated GPS measurements. Tectonophysics, v. 294(3), pp. 237-252.

Kebeasy, R., 1990, Seismicity. In: Said R. (ed.), Geology of Egypt. Balkema, Rotterdam, 51-59 p.

Klinger, Y., Avouac, J. P., Abou Karaki, N., Dorbath, L., Bourles, D., and Reyss, J. L., 2000, Slip rate on the Dead Sea transform fault in northern Araba valley (Jordan). Geophysical Journal International, v. 142(3), pp. 755-768.

Kreemer, C., Holt, W. E. and Haines, A. J., 2003, An integrated global model of present-day plate motions and plate boundary deformation. Geophysical Journal International, v. 154(1), pp.

8-34.

Le Pichon, X. and Gaulier, J. M., 1988, The rotation of Arabia and the Levant fault system. In: Le Pichon, X., Cochran, J.R. (Eds.), The Gulf of Suez and Red Sea Rifting. Tectonophysics v. 153, pp. 271-294.

Lyberis, N., 1988, Tectonic evolution of the Gulf of Suez and Gulf of Aqaba. Tectonophysics, v. 153, pp. 209-220.

Mahmoud, S. M., 2003, Seismicity and GPS-derived crustal deformation in Egypt. Journal of Geodynamics, v. 35, pp. 333-352.

Mahmoud, S., Reilinger, R., McClusky, S., Vernant, P., and Tealeb, A., 2005, GPS evidence for northward motion of the Sinai Block: Implications for E. Mediterranean tectonics. Earth and Planetary Science Letters, v. 238(1), pp. 217-224.

McClusky, S., Balassanian, S., Barka, A., Demir, C., Ergintav, S., Georgiev, I., Veis, G., et al., 2000, Global Positioning System constraints on plate kinematics and dynamics in the eastern Mediterranean and Caucasus. Journal of Geophysical Research: Solid Earth, v. 105(B3), pp. 5695-5719.

McClusky, S., Reilinger, R., Mahmoud, S., Ben Sari, D. and Tealeb, A., 2003, GPS constraints on Africa (Nubia) and Arabia plate motions. Geophysical Journal International, v. 155(1), pp. 126-138.

McKenzie, D. P., 1972, Active tectonics of the Mediterranean Region, Geophysical Journal Royal Astronomical Society, v. 30, pp. 109-185.

Moretti, I. and Colletta, B., 1987, Spatial and temporal evolution of the Suez rift subsidence, Journal of Geodynamics, v. 7, pp. 151-168.

Morsy, M. A., Hady S.E., and El-Meneam E. A., 2012. Source parameters of some recent earthquakes in the Gulf of Aqaba, Egypt. Arabian Journal of Geoscience, v.5 (5), pp. 943-952.

Moustafa, A. R., 1996, Internal structure and deformation of an accommodation zone in the northern part of the Suez rift. Journal of Structural Geology, v. 18, pp. 93-107.

Omar, G. I. and Steckler, M.S., 1995, Fission-track evidence on the initial rifting of the Red Sea: two pulses, no propagation. Science, v. 270, pp. 1341–1344.

Patton, T. L., Moustafa, A. R., Nelson, R. A., and Abdine, S. A., 1994, Tectonic evolution and structural setting of the Suez Rift, American Association of Petroleum Geologists Memoir, pp. 9-9.

Reilinger, R., McClusky, S., Vernant, P., Lawrence, S., Ergintav, S., Cakmak, R., Karam, G., et al., 2006, GPS constraints on continental deformation in the Africa-Arabia-Eurasia continental collision zone and implications for the dynamics of plate interactions. Journal of Geophysical Research: Solid Earth, v. 111(B5).

Riguzzi, F., Pietrantonio, G., Piersanti, A., and Mahmoud, S. M., 2006, Current motion and short-term deformations in the Suez–Sinai area from GPS observations. Journal of Geodynamics, v. 41(5), pp. 485-499.

Salamon, A., Hofstetter, A., Garfunkel, Z., and Ron, H., 2003, Seismotectonics of the Sinai subplate–the eastern Mediterranean region. Geophysical Journal International, v. 155(1), pp. 149-173.

Saleh, S., Jahr, T., Jentzsch, G., Saleh, A. and Ashour, N. M., 2006, Crustal evaluation of the northern Red Sea rift and Gulf of Suez, Egypt from geophysical data: 3-dimensional modeling. Journal of African Earth Sciences, v. 45(3), pp. 257-278.

Steckler, M. S., Berthelot, F., Lyberis, N. and Le Pichon, X., 1988, Subsidence in the Gulf of Suez: implications for rifting and plate kinematics.Tectonophysics, v. 153(1), pp. 249-270.

Steckler, M.S., 1985, Uplift and extension at the Gulf of Suez: indications of induced mantle convection. Nature, v. 317, pp. 135-139.

Steckler, M. S., Feinstein, S., Kohn, B. P., Lavier, L. L. and Eyal, M., 1998, Pattern of mantle thinning from subsidence and heat flow measurements in the Gulf of Suez: Evidence for the rotation of Sinai and along-strike flow from the Red Sea. Tectonics, v. 17(6), pp. 903-920.

Steckler, M. S. and ten Brink, U.S., 1986, Lithospheric strength variations as a control on new plate boundaries: examples from the northern Red Sea Region. Earth and Planetary Science Letters, v. 79, pp. 120-132.

Strecker, M. R. and Bosworth, W., 1991, Quaternary stress-field change and rifting processes in the East African Gregory Rift. EOS, Transactions of American Geophysical Union, v. 72, pp. 17-22.

Taha, R., and Miguel, M., 2008, A tectonic model of the Sinai Peninsula based on magnetic data. Journal of Geophysics and Engineering, v. 5(4), pp. 469.

Wdowinski, S., Bock, Y., Baer, G., Prawirodirdjo, L., Bechor, N., Naaman, S., Knafo, R. Forrai, Y. and Melzer, Y., 2004, GPS measurements of current crustal movements along the Dead Sea Fault. Journal of Geophysical Research: Solid Earth, v. 109(B5).

Wessel, P. and Smith, W. H. F., 1995, New version of the generic mapping tools released: EOS Trans. AGU, v. 76(33), pp. 329.

Westaway, R., 1994, Present-day kinematics of the Middle East and eastern Mediterranean. Journal of Geophysical Research, 99, 12071-12090.

Zheng, Z., Kemeny, J. and Cook, N. G. W., 1989, Analysis of borehole breakouts. Journal of Geophysical Research, v. 94, pp. 7171-7182.

Zoback, M. L., 1992, First and second order pattern of stress in the lithosphere: the world stress map project. Journal of Geophysical Research, v. 97, pp. 11703-11728.

Zoback, M. L. and Zoback, M. D., 1980, State of stress in the conterminous United States. Journal of Geophysical Research, v. 85, pp. 6113-6156.